SOCIETY FOR SCIENCE AND EDUCATION
UNITED KINGDOM

TNC TRANSACTIONS ON NETWORKS AND COMMUNICATIONS

VOLUME 6, NO. 6
ISSN: 2054 -7420

Mitigation of Terrain Effects using Beamforming Antennas in Ad Hoc Networks

Vinay B. Ramakrishnaiah, Robert F. Kubichek, and Suresh S. Muknahallipatna
Department of Electrical and Computer Engineering, University of Wyoming, United States;
sureshm@uwyo.edu

ABSTRACT

Wireless communication is sensitive to ambient noise as well as interference due to the use of a shared medium. The link quality is significantly affected by the surrounding terrain including buildings, hills, foliage, etc. Terrain changes also pose a problem for communication and localization in mobile ad-hoc networks and in the deployment of Internet of Things (IoT). Many of these problems can be addressed through careful antenna design, but these can be challenging as they require complex hardware and software. We propose a new approach called virtual terrain leveling (VTL), which acts as a trade-off between the complex antenna design approaches and the simple omni-directional antennas. VTL virtually nullifies the effects of the terrain using phased array antennas to compensate for the path losses. Convex optimization and the Nelder-Mead simplex method are used to compute the antenna array weights that minimize the error between the ideal and achieved beam patterns. Simulations are performed in the presence of different terrains and the received power at varying distances from the transmitter is analyzed. The results show improved received power up to a specified distance from the transmitter and then power decays rapidly with increasing distance, indicating interference reduction.

Keywords: Terrain nullification, Phased arrays, Convex optimization, Nelder-Mead optimization.

1 Introduction

Unlike wired communication, wireless communication is sensitive to ambient noise as well as interference due to the use of a shared medium. Wireless spectrum is a scarce resource, which makes it impractical for large wireless ad hoc networks to carry out simultaneous transmissions using only frequency division techniques. Therefore, the signal transmissions are separated in space, time, and encoding to facilitate increased simultaneous transmissions. These interference avoidance techniques usually require a-priori planning and centralized control. Increase in the number of nodes exacerbates the interference issue and makes the design of centralized control more difficult.

Signal quality in wireless networks is significantly affected by the surrounding terrain including buildings, hills, foliage, etc. Terrain features pose difficult challenges to implementation of mobile ad hoc networks (MANETs). The performance of MANETs and how they are influenced by their ability to cope with topology changes arising from node mobility under the influence of terrain is analyzed in [1]. They find that the probability of two connected nodes remaining connected falls rapidly as the line-of-sight (LOS) probability

DOI: 10.14738/tnc.66.5481
Publication Date: 12nd December 2018
URL: http://dx.doi.org/10.14738/tnc.66.5481

decreases. Also, most of the routing protocols are designed based on the assumption of omni-directional transmissions, which is unlikely to hold for terrain encountered in most practical applications.

Beamforming antennas can effectively address the interference issue, even without a central control, acting as a spatial filter by directing the beam in certain directions. They create radiation patterns by adding the signals constructively in desired directions and destructively in others. The antenna beam synthesis techniques are marginally addressed for fixed infrastructure networks in previous literature. [2] uses a simplified sector model for antenna beams to approximate azimuth beams. [2] [3] use a simplified cellular model by neglecting the topography. In [4] a coverage goal is defined, and the amount of power radiated outside the cell is compared with the amount of power radiated within the cell. But they use the same approximation as in [2], which does not consider the topography. Smart antenna solutions including switched beam antennas, adaptive beam arrays, and Multiple-Input Multiple-Output (MIMO) systems [5] usually require a separate transceiver behind every antenna element. This is problematic for large antenna array systems as they are expensive and also because of the requirement of high speed Analog-to-Digital / Digital-to-Analog converters to accommodate the necessary bandwidth. Several signal processing techniques like randomization and cancellation are used to reduce inter-cell interference. These techniques try to average the interference across the system bandwidth and null out certain directions. The required processing power and complexity of these advanced techniques limit their use in wireless ad hoc networks.

[6] [7] [8] describe phase-only antenna arrays that achieve optimal beam patterns with maximum average network signal-to-noise ratio (SNR). They use a hybrid analog/digital beamformer to steer the antenna beams using a single transceiver, power splitter/combiner, and electronically controlled analog phase shifters. These solutions are independent of the path loss models, therefore, making it easy to incorporate any terrain or traffic information. However, they are computationally complex requiring a centralized computer to pre-compute the antenna weights. A second order cone programming and semi-definite programming based approach to solve the array synthesis problem in non-uniform array with constraints on the magnitude is presented in [9]. They also address the robust array pattern synthesis in the presence of gain and phase uncertainties.

In [10], we presented a preliminary analysis of Virtual Terrain Leveling (VTL) that acts as a trade-off between the complex antenna design approaches and the simple omni-directional antennas. VTL uses the hybrid analog/digital beam forming technique to limit the radiated power and validates the free space assumption by nullifying the effects of terrain up to a specified range from the transmitter. In other words, phased array antennas are used that provide gain inversely proportional to the path loss. In this paper, we extend our analysis to include active array antennas, and also study different array sizes and geometries. The antenna beams are synthesized using two different approaches, i.e., convex optimization [11] and the Nelder-Mead simplex method [12]. The idea behind VTL relies on efficiently pre-computing the radio propagation maps using a suitable path loss model and using this information to find the antenna array weights at the transmitter. Approximation methods such as the ones presented in [13] [14] can be used to get a low complexity representation of radio propagation maps for VTL implementation. We show that VTL can mitigate issues by providing near omni-directional propagation in the presence of terrain with the use of directional antennas and limiting the range of the radiated signal to reduce interference and to increase frequency reuse. With the use of pre-computed radio propagation maps, VTL can avoid deafness in MANETs as they will be able to hear their neighboring nodes from all directions.

This paper is organized as follows: Section 2 explains the VTL methodology and the goals of this research. In Section 3, background theory on phased array antennas, the array gain, and the optimization methods used to obtain array gain patterns is discussed. The simulations and analysis of results of the proposed VTL approach is presented in Section 4. Section 5 provides a summary of this research work and concludes the paper.

2 VTL Methodology

In many antenna applications, the problem of antenna pattern synthesis is of extreme importance and therefore it has been studied for decades. However, most of the existing literature assumes the knowledge of the optimal beam pattern and uses some kind of optimization algorithm to solve for system parameters. For example, the authors of [15] assume a desired, synthetic complex array amplitude vector, comprised of ones and zeros, where 1s correspond to the directions of interest, and compute the amplitude weights that minimize the error between the realized beam pattern and the synthetic complex array amplitude vector. Similarly, [16] uses genetic algorithm to search for complex roots that provide nulls in the desired directions. Particle-swarm optimization is used in [17] to search for the optimal array geometry that can realize the main beam with the desired beam width, providing unity gain in the directions of interest. Through VTL, we provide an analytical approach for computing the antenna gain patterns that minimizes the effects of path loss. The analytical approach eliminates the need for speculative beam patterns based on the synthetic complex array amplitude vectors.

VTL virtually nullifies the effects of terrain at a desired distance from the transmitter by increasing the gain in the directions of increased path loss. Typically, the transmitter power is set to provide radio coverage up to a certain virtual radius (VR) based on receiver sensitivity. The idea is to reduce the transmitter power and use an antenna array with a gain distributed in such a way that it compensates for the lower received power. To illustrate the concept, consider a simple wireless network without adaptive power control, whose network protocol assumes homogeneous terrain with equal propagation in all directions. Unfortunately, real-world terrain causes significant variation in propagation distance depending on direction, which impairs network efficiency. In this example, assume the desired “cell radius” is 1 km and that transmitter power P_t has been adjusted so that all locations in the cell are within range of the base station as shown in the cartoon of Figure. 1 (a). By satisfying the worst-case direction of 200°, we see excessive range of over 2 km in other directions, likely causing interference in adjacent cells. VTL uses a passive antenna beam pattern that is inversely related to range, using less gain in some directions in order to provide higher gain in others, as shown in Figure. 1 (b). Figure. 1 (c) shows the range map after VTL is applied. The reason the corrected range map is not an ideal flat line is because a practical antenna array cannot perfectly remove all effects of loss-vs-direction. After VTL is applied, it is clear that the resulting system has excess range, and transmitter power can be reduced while maintaining the desired 1 km cell radius, as shown in Figure. 1 (d). VTL thus gives better power efficiency, reduced adjacent cell interference, and improved frequency reuse.

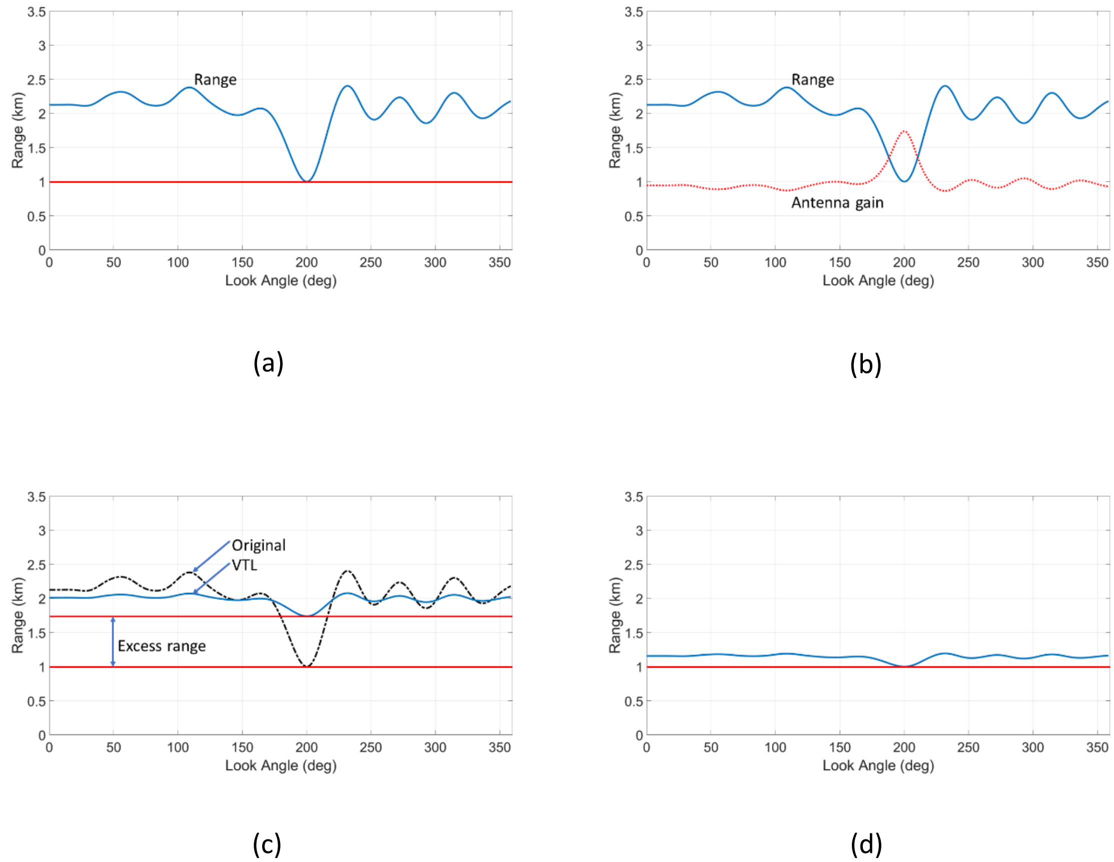

Figure. 1: VTL cartoon showing (a) Range vs. angle, minimum range = 1 km. (b) Antenna gain pattern (not to scale). (c) Range with VTL. (d) Range after VTL, reduced transmitter power.

We make use of the Cost 231 Walfisch-Ikegami model (WIM) [18] [19] to demonstrate the concept of VTL. The WIM provides a theoretical model for urban communication systems. In this model, the rows or blocks of buildings are viewed as diffracting cylinders. Buildings are treated as absorbing screens, which reduces the propagation process to multiple forward diffractions past a series of screens. Diffraction is contemplated right from rooftops down to street level, which provides path loss predictions close to average measurement path loss.

For an omnidirectional antenna, if a free line-of-sight (LOS) exists in an urban canyon, the path loss in decibels is given by

$$L_{\mathrm{WIM}} = 42.6 + 20\log f + 26\log R,$$

where the frequency f is given in MHz and R is the range in km. If there is no LOS path between the transmitter and receiver, the path loss is defined as

$$L_{WIM} = \begin{cases} L_{FS} + L_{rts} + L_{msd} & \\ L_{FS}, & if\ L_{rts} + L_{msd} < 0, \end{cases}$$

where L_{FS} is the free-space path loss. The coupling of the wave propagating along the multi-screen path into the receiver located in the street is defined as the rooftop-to-street diffraction and scatter loss, L_{rts} given by

$$L_{rts} = \begin{cases} -16.9 - 10\log w + 10\log f + 20\log \Delta h_{receiver} + L_{ori}, & if\ h_{roof} > h_{receiver} \\ 0, & if\ L_{rts} < 0 \end{cases}$$

where L_{ori} is the street orientation loss defined as

$$L_{ori} = \begin{cases} -10 + 0.354\psi & for\ 0 \leq \psi < 35 \\ 2.5 + 0.075(\psi - 35) & for\ 35 \leq \psi < 55. \\ 4 - 0.114(\psi - 55) & for\ 55 \leq \psi \leq 90 \end{cases}$$

Here, ψ is the angle in degrees between the base station and the road. The multiscreen diffraction loss L_{msd} is given by

$$L_{msd} = L_{bsh} + k_a + k_d \log R + k_f \log f - 9\log b,$$

where

$$L_{bsh} = \begin{cases} -18\log(1 + \Delta h_{base}) & for\ h_{base} > h_{roof} \\ 0 & for\ h_{base} \leq h_{roof} \end{cases},$$

$$k_d = \begin{cases} 18 & for\ h_{base} > h_{roof} \\ 18 - 15\dfrac{\Delta h_{base}}{h_{roof}} & for\ h_{base} \leq h_{roof} \end{cases},$$

$$k_a = \begin{cases} 54 & for\ h_{base} > h_{roof} \\ 54 - 0.8\Delta h_{base} & for\ R \geq 0.5\ km\ and\ h_{base} \leq h_{roof} \\ 54 - 1.6\Delta h_{base} R & for\ R < 0.5\ km\ and\ h_{base} \leq h_{roof} \end{cases},$$

and

$$k_f = -4 + \begin{cases} 0.7\left(\dfrac{f}{925} - 1\right) & suburban\ areas \\ 1.5\left(\dfrac{f}{925} - 1\right) & urban\ areas \end{cases}.$$

The predicted power received at a receiver can be computed using the WIM as

$$P_{rWIM}(\theta) = \frac{P_t G_t(\theta) G_r(\theta)}{L_{WIM}(\theta)},$$

where P is the power, $G(\theta)$ is the antenna gain, $L_{WIM}(\theta)$ is the path loss, and the subscripts indicate the association of the quantities with either the transmitter or the receiver. This compares with the predicted loss in a free-space environment

$$P_{rFSM}(\theta) = \frac{P_t G_t(\theta) G_r(\theta)}{L_{FSM}},$$

where $L_{FSM} = \left(\frac{4\pi R}{\lambda}\right)^2$. Here, λ is the wavelength, and R is the distance from the transmitter in meters. Using omni-directional antennas for both the transmitter and receiver, the power received can be written as $P_{rWIM}(\theta) = \frac{P_t}{L_{WIM}(\theta)}$, and $P_{rFSM} = \frac{P_t}{L_{FSM}}$.

VTL tries to find the transmitter antenna gain such that $P_{rWIM}(\theta) = P_{rFSM}$, i.e.,

$$\frac{P_t G_t(\theta)}{L_{WIM}(\theta)} = \frac{P_t}{L_{FSM}}$$

or

$$G_t(\theta) = \frac{L_{WIM}(\theta)}{L_{FSM}}, \qquad (1)$$

where L_{FSM} is the free space path loss. Equation (1) provides an analytical solution for finding the gain pattern that compensates for the propagation path losses. The solution works regardless of the path loss model used. Also, it is important to notice that the antenna gain obtained using equation (1) is the power gain of the antenna. Therefore, the antennas/antenna arrays have to be designed such that they closely match this desired power pattern subject to the design constraints like system power, degrees of freedom, etc. In case of very high path losses, it is beneficial to include the condition $L_{WIM} = \min(L_{WIM}, Maximum\_Loss\_Threshold)$ to prevent futile gain in the directions of very high path loss.

3 Background Theory

3.1 Antenna Arrays

Antenna arrays are effective in providing a flexible and efficient way to synthesize antenna gain patterns. The power radiated or received by the antenna is enhanced in certain directions and diminished in others by addition and cancellation of power. For VTL, a low complexity hybrid analog/digital beamforming antenna described in [6] is used. This system uses a single transceiver along with digitally controlled phase shifters and step attenuators/amplifiers as shown in Figure. 2.

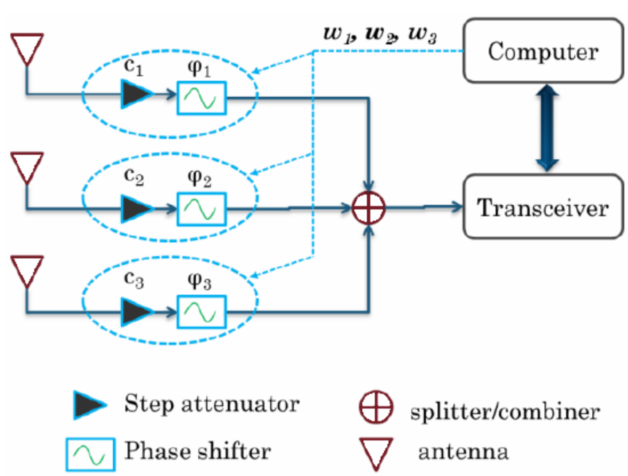

Figure. 2: Low complexity hybrid analog/digital beamformer.

In the hybrid system, the complex antenna weights, w_k are applied by a computer to the receiver outputs to form the desired antenna beams. For a generic system, the antenna weights $w_k = c_k e^{j\phi_k}$, have both magnitude and phase. The complexity of the antenna system can be further reduced by eliminating the step attenuator/amplifier, which will constrain the weights to be phase-only ($w_k = e^{j\phi_k}$).

The transmitted signal can be represented as $r(t) = 2s(t)\cos(\omega_0 t) = s(t)e^{j\omega_0 t} + s(t)e^{-j\omega_0 t}$, where $\omega_0 = 2\pi f_0$ is the angular frequency. The block diagram of the receiver is shown in Figure. 3.

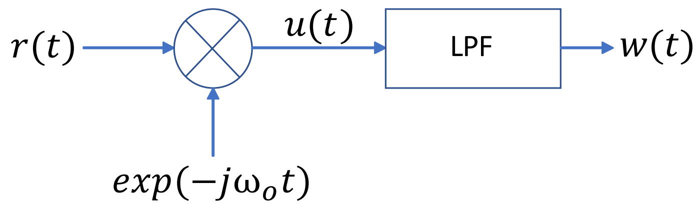

Figure. 3: Block diagram of the receiver.

The mixer output signal $u(t) = s(t)e^{-2j\omega_0 t} + s(t)e^{0}$, but the high frequency component is removed by the low pass filter giving $w(t) = s(t)$. Therefore, we can safely assume the transmitter signal to be $r(t) = s(t)e^{j\omega_0 t}$ to avoid unnecessary calculations.

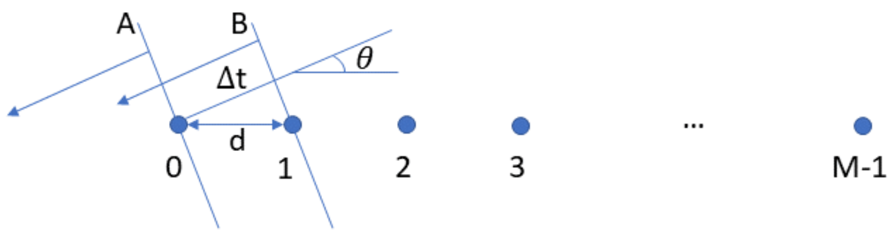

Figure. 4: M-element uniform linear array.

A uniform linear array consisting of M antenna elements is shown in Figure. 4. Consider a single instant of time t, giving a snapshot of the wavefront for a signal arriving from direction θ. By looking at Figure. 4, it is evident that wave B touches antenna #1 before it touches antenna #0. Let the wavefront at antenna #0 be $s_0(t) = s(t)e^{j\omega_0 t}$, then the wavefront at antenna #1 is $s_1(t) = s_0(t + \Delta t)$. We assume a "low-pass narrow-band" signal $s(t)$ with bandwidth << f_0. Therefore, $s(t + \Delta t) \approx s(t)$, where $\Delta t = \frac{d cos\theta}{c}$ and $c = \lambda f_0$. Therefore $\Delta t = \frac{2\pi d cos\theta}{\omega_0 \lambda}$. The signal received at the receiver for antenna m is given as $r_m \simeq s(t)e^{j\omega_0(t+m\Delta t)} = s(t)e^{j\omega_0\left(t+\frac{2\pi m d cos\theta}{\omega_0\lambda}\right)}$. For the entire array, the received signal will be $\boldsymbol{r}(t) = s(t)e^{j\omega_0 t}\left[1, e^{jkdcos\theta}, e^{j2kdcos\theta}, \dots\right]^T$, where $k = \frac{2\pi}{\lambda}$ is the wavenumber.

The received signal is represented as $r(t) = s(t)\cos(\omega_0 t) + v(t)$, where $s(t)$ is a narrow band message signal and $v(t)$ is the white noise. The receiver down-converts the signal resulting in a complex base-band signal $\boldsymbol{y}(t)$. For example, the result for a uniform linear array is

$$\boldsymbol{y}(t) = \begin{bmatrix} 1 \\ e^{jkdcos\theta} \\ \vdots \\ e^{j(M-1)kdcos\theta} \end{bmatrix} s(t) + \begin{bmatrix} v_0(t) \\ \vdots \\ v_{M-1}(t) \end{bmatrix}$$

or $\boldsymbol{y}(t) = \boldsymbol{h}(\theta)s(t) + \boldsymbol{V}$, where k, d, and θ are the wavenumber, antenna element separation, and direction of arrival (DOA), respectively, and $\boldsymbol{h}(\theta)$ is called the steering vector. Note that $\boldsymbol{h}(\theta)$ must be modified for each specific antenna array geometry to give proper delay characteristics in the direction θ. It is possible to find a filter $\boldsymbol{K}$ that amplifies the signals in certain directions. Therefore, in case of antenna arrays the term $\boldsymbol{K}^*\boldsymbol{h}(\theta)$ represents the array gain.

3.2 Power Gain of Antenna Arrays

Antenna arrays act as directional amplifiers, with a voltage amplification factor of $\boldsymbol{K}^*\boldsymbol{h}(\theta)$, also known as the Array Factor (AF), which is a function of θ (assuming 2D patterns). The coefficients of the filter $\boldsymbol{K}$ are the antenna weights $\boldsymbol{w} = [w_0, w_{\boldsymbol{1}}, \dots, w_{M-1}]^T$, therefore, $AF = \boldsymbol{w}^T\boldsymbol{h}(\theta)$. Most of the literature like [6] [11] [15] [20] [21] considers the antenna array gain to be equal to either the array factor or the power gain, $G_p(\theta, \phi) = |AF(\theta, \phi)|^2 G(\theta, \phi)$, where $G(\theta, \phi)$ is the power gain of a single element of the array. These representations of the antenna gain provide accurate directional characteristics and signal-to-noise ratios (SNRs) but fail to preserve the actual power amplification provided by the antenna. The array factor provides the complex amplitude gain for an array and does not directly relate to the power gain. The solution to this problem is addressed in [22]. They show that the power gain of an antenna array is

$$G_p(\theta) = 2\pi \frac{|AF(\theta)|^2}{\int_0^{2\pi} |AF(\theta)|^2 \, d\theta} P_{fact}. \tag{2}$$

where $P_{fact} = \frac{1}{M}\sum_{j=0}^{M-1} |w_j|$, and M is the number of antennas in the array.

In order to synthesize the antenna array beam pattern, the two parameters that can be modified are the antenna weights, $\boldsymbol{w}$ and the steering vector, $\boldsymbol{h}(\theta)$. As shown in section 3-A, the steering vector is dependent on the antenna array geometry and is fixed for a given antenna array. The flexibility of antenna arrays lies within the fact that complex antenna weights can be modified to obtain the desired beam pattern.

There are several ways to find the weight vector, $\boldsymbol{w}$. For example, it is possible to find $\boldsymbol{w}$ that minimizes the output noise power while holding unit gain in the signal direction. This is called the "Minimum Variance Distortion-less Response" filter. Numerous other beam synthesis techniques like the Schelkunoff polynomial method [23], Fourier transform method [24], Woodward-Lawson method [25] [26], etc. have been extensively studied over the years. The problem with most of the methods is that there is no absolute guarantee the solution is globally optimal unless the problem is convex [27] [28], and they also assume the knowledge of the noise covariance matrix, which requires complex and expensive hardware for realization.

In this paper, we use the convex optimization [11] technique for synthesizing beam patterns for design problems that are convex. However, the problem of computing phase-only weights is non-convex; therefore, the Nelder-Mead simplex search [12] is also used for minimizing the desired fitness function in such cases.

3.3 Convex Optimization

A set, C is convex [11] if and only if for any two points $x_1, x_2 \in C$ and any θ where $0 \leq \theta \leq 1$, the point $\theta x_1 + (1 - \theta)x_2$ also is an element of C. In other words, this means that a set is convex if the direct path between any two points in the set is entirely included in the set. For a function f, if the line segment between $(x, f(x))$ and $(y, f(y))$, which is a chord from x to y, lies above the graph of f, then the function is defined to be convex. Mathematically, a function f is convex on a convex domain if for all $x, y \in \mathbf{dom}\, f$, and θ with $0 \leq \theta \leq 1$, the following inequality holds:

$$f(\theta x + (1-\theta)y) \leq \theta f(x) + (1-\theta)f(y). \tag{3}$$

The convex optimization problem involves minimizing the convex function over its domain, which is a convex set. The convex optimization problem is defined using the following notation, which is often referred to as disciplined convex programming [29] [30]:

$$\begin{aligned} & minimize\ f_0(x) \\ & subject\ to\ f_i(x) \leq 0, \quad i = 1, \dots, m \\ & \qquad\qquad h_i(x) = 0, \quad i = 1, \dots, p \end{aligned} \tag{4}$$

and the objective is to find the value x that minimizes $f_0(x)$ satisfying $f_i(x) \leq 0, i = 1, \dots, m$, and $h(x) = 0,\ \ i = 1, \dots, p$. It is always possible to find the global minima of convex functions as the local minima itself is the global minima as per the definition of convex functions. Many optimization problems like least squares techniques, linear programming, conic optimization, etc., fall into the category of convex optimization, and computing the weights of an antenna array can be treated as a convex problem by relaxing the constraints.

3.4 Nelder-Mead Simplex Method

While the convex optimization approach of computing the optimal antenna weights finds solutions with relaxed constraints, it requires using step attenuators or amplifiers that increases the hardware cost and complexity of the antenna system. Therefore, it is sometimes desirable to find antenna weights that are phase-only, so that the system could be realized using only the phase shifters. However, constraining the weights to have unit magnitude makes the optimization problem to be non-convex as discussed previously. Hence, we make use of the Nelder-Mead algorithm to perform an unconstrained search for phase-only weights.

The Nelder-Mead (NM) algorithm [12] is one of the most widely used methods for non-linear unconstrained optimization. The Nelder-Mead method attempts to minimize a scalar valued non-linear function of n variables using only the function values without any derivative information. This algorithm uses a simplex of n-dimensional vectors $\boldsymbol{x}$. Let x_i, denote the list of points in the current simplex, with $i = 1, \dots, n+1$. Our objective is to minimize the function f such that $\boldsymbol{x} \in \mathbb{C}^{\boldsymbol{n}}$ is the domain of f, therefore, x_i is referred to as the best point, and x_{n+1} as the worst point. Four scalar parameters $reflection\ (\rho), expansion\ (\chi), contraction\ (\gamma)$, and $shrinkage\ (\sigma)$ are specified for Nelder-Mead method.

The following indicates one iteration of the Nelder-Mead algorithm [31]:

- The $n+1$ vertices are ordered such that $f(x_1) \leq f(x_2) \leq \cdots \leq f(x_{n+1})$.
- The reflection point, x_r is computed as $x_r = \bar{x} + \rho(\bar{x} - x_{n+1}) = (1-\rho)\bar{x} - \rho x_{n+1}$, where $\bar{x} = \sum_{i=1}^{n} \frac{x_i}{n}$. Evaluate $f_r = f(x_r)$. If the value $f_1 \leq f_r \leq f_n$, the reflection point x_r is accepted and the iteration terminates.

- The expansion point is computed as $x_e = \bar{x} + \chi(x_r - \bar{x}) = \bar{x} + \rho\chi(\bar{x} - x_{n+1}) = (1 + \rho\chi)\bar{x} - \rho\chi x_{n+1}$, if $f_r < f_1$ and the value of the function f_e at x_e is evaluated. The iteration is terminated after retaining either x_e $(f_e < f_r)$ or x_r $(f_e > f_r)$.
- Contraction is performed by computing the contracted point $x_c = \bar{x} + \gamma(x_r - \bar{x})$. A new simplex is obtained by using the contracted point, x_c, if it is better than the worst point.
- The function is evaluated by replacing all the points by $v_i = x_1 + \sigma(x_i - x_1)$, $i = 2, \ldots, n+1$, except for the best point. The new vertices $x_1, v_2, \ldots, v_{n+1}$ are used for update in the next iteration.

4 Simulation Results and Analysis

The simulations were performed in Matlab with the following system parameters. The WIM was used to compute the path losses with a base station height of 50 m, receiver height of 3 m, and the frequency of operation was set to 900 MHz. The building heights and street widths were varied according to the desired terrain. Different antenna array geometries were tested, and the antenna weights computed using convex optimization and NM simplex method were compared.

The optimal antenna weights can be found by minimizing the squared error between the gain pattern that compensates for the path losses as given by equation (1) and the estimate of the gain obtained using the antenna with limited degrees of freedom. The constraint on the weights, $\boldsymbol{w}$ determines the requirement of amplifiers or attenuators in the system. For example, if the magnitude of the weights is constrained to be less than or equal to 1, then the system could be realized using only phase shifters and attenuators without the need for amplifiers. On the other hand, having fixed constraints for magnitudes (phase-only weights) makes the optimization problem to be non-convex. The optimization problem for finding the optimal antenna weights using convex optimization was set up as follows:

$$\xi(\theta) = \boldsymbol{w}^T \boldsymbol{h}(\theta) - \sqrt{G_t(\theta)} \tag{5}$$

$$minimize \ \|\boldsymbol{\xi}\|_2$$

$$subject\ to \ |w_i| \leq 1, \quad i = 0, \ldots, M-1$$

In our simulations, a 2-norm penalty function is used to penalize the errors. If the function f is a norm function and $0 \leq \theta \leq 1$, then from triangle inequality, $\|\theta x + (1-\theta)y\| \leq \|\theta x\| + \|(1-\theta)y\| = \theta\|x\| + (1-\theta)\|y\|$ is true, where the equality follows from homogeneity of a norm. Therefore, the norm function satisfies equation (1) and is convex by definition. Hence, we can solve for the antenna weights using standard convex optimization solvers.

The solutions developed in this paper uses CVX [32] [33], which is a Matlab based modelling system for convex optimization. CVX supports disciplined convex programming [29] [30], where the objective functions and constraints are identified as convex from the outset of the problem and can be specified as standard Matlab expressions.

To enforce the phase-only constraint, the NM simplex method was used to find the optimal value of the weights that minimizes the absolute value of error between the desired gain obtained using equation (1) and the achieved gain. The problem was set up as follows – the phase-only weights of the antenna array are given by

$$\boldsymbol{w} = e^{j\boldsymbol{\phi}}, \tag{6}$$

where $\boldsymbol{\phi} = [\phi_1, \phi_2, \dots]$ are the individual antenna phases. The estimate of the gain with limited degrees of freedom is computed as $G_{est}(\theta) = |\boldsymbol{w}^T \boldsymbol{h}(\theta)|^2$, and the objective function is defined as

$$\xi = \frac{1}{n}\sum_{i=1}^{n} |G_t(\theta_i) - G_{est}(\theta_i)|. \tag{7}$$

The error function $f = \xi$ is minimized using the NM algorithm to find the optimal value of antenna weights. The antenna weights will be constrained to be phase-only due to the way in which the weights are defined in equation (6), i.e., setting the magnitude to be unity. The results in this paper are developed using Matlab's implementation of the NM algorithm utilized through the $fminsearch()$ function.

Using the suburban terrain setting, a circular antenna array with 36 elements was used and the achieved gain pattern was compared with the ideal desired pattern. Figure. 5 shows the ideal and the achieved gain patterns using the convex optimization and the NM simplex approach. The ideal gain pattern computed using equation (1) is used to compensate for path losses and makes the terrain apparently flat for radio communication at the VR. However, the ideal gain requires very high power for realization (Figure. 5: $\frac{1}{2\pi}\times$(Area under the blue curve in Watts)), and therefore, is not practical. Hence, the achieved gain pattern of a passive array can only achieve the desired directivity (shape), but does not meet the power amplification level as shown in Figure. 5. The achieved gain pattern shows increased directivity in the desired directions while conserving the total power of the system to be equal to the transmitter power (passive antenna gain). We can see from Figure. 5 that the convex optimization approach provides a smooth pattern compared to the NM approach that tries to enforce the phase-only constraint at the optimization stage.

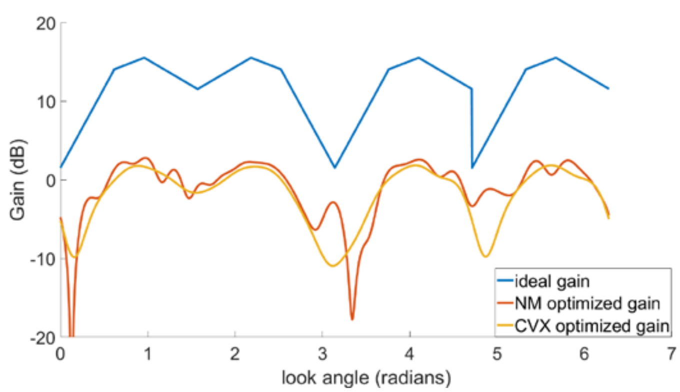

Figure. 5: Ideal and achieved beam patterns.

The power received using the achieved gain pattern in the suburban setting at a distance of 1 km from the transmitter is shown in Figure. 6, and is compared with the received power using an omni-directional antenna for transmission. A 10 W transmitter is used, and the WIM to compute the path losses. Figure. 6 shows that VTL tries to provide a flat response by directing the gain towards increased path losses. Also, the power received with the CVX optimized array has a lower but smoother response due to the relaxed optimization constraints compared to the NM optimized array that constrains the weights to be phase-only. The convex optimization approach constrains the weights to be less than or equal to one. In other words, the weights are realized using step attenuators in hardware. That is why the power received from the CVX optimized array is lower than the power received from the phase-only NM array, which does not use any attenuators.

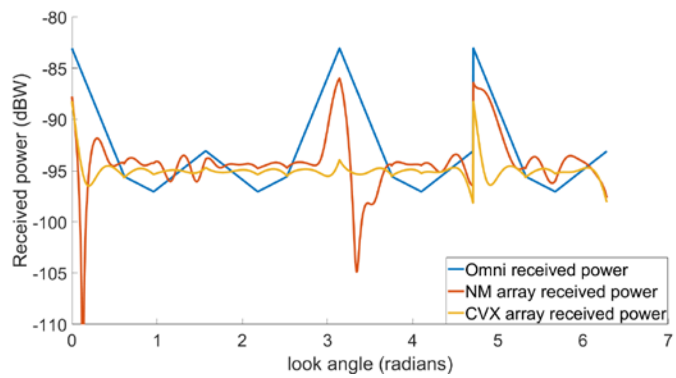

Figure. 6: Received power at a distance of 1 km from the transmitter.

As a measure of performance, the percentage of look-angles above the threshold of -95 dBW is plotted as a function of distance and is shown in Figure. 7. The threshold of -95 dBW was arbitrarily chosen to represent the sensitivity of modern receivers. VTL tries to increase the power received up to the VR from the transmitter. In our simulations, the VTL power gain was computed to achieve a uniform response up to a distance of 1 km from the transmitter. It can be seen from Figure. 7 that the received power with VTL is higher than the received power with omni-directional antennas up to 1.05 km. The power rapidly drops with increasing distances, which is a desirable behavior to avoid interference and for better frequency reuse in wireless networks. Therefore, with VTL, fixed infrastructures like cell-phone base stations will be able to provide increased reception within the cell, at the same time reducing interference to the neighboring cells.

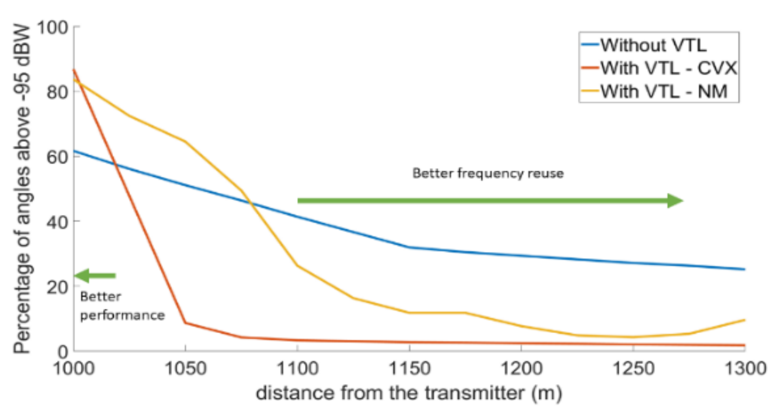

Figure. 7: Percentage of look angles above the threshold of -95 dBW for arrays optimized using different techniques as the distance from the transmitter varies.

Further, the variation of the percentage of look-angles as a function of total power was examined and is shown in Figure. 8. The performance of the VTL antenna system with weights computed using either the CVX or NM approach is evaluated using the power injected into antenna system and the corresponding signal power delivered to the receiver. With very low transmitter powers (less than 6 W), the percentage of angles below the threshold with VTL is less than the percentage of angles below the threshold with omni-directional transmission. This is because, VTL tries to provide a flat gain pattern rather than increasing the coverage of signals above the desired threshold. As the transmitter power increases, the response with VTL gets significantly better. We can also see that the relaxed constraint system using convex optimization for finding the weights provide slightly better response than the NM optimized arrays with fixed constraints.

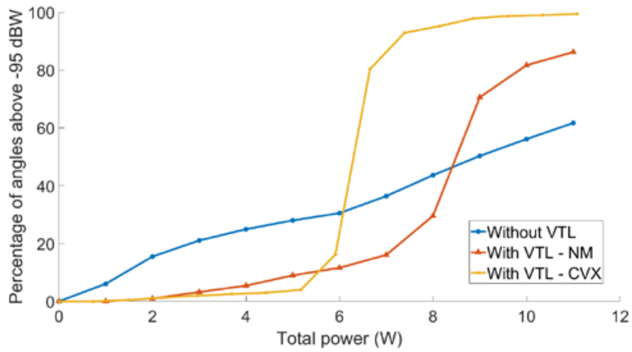

Figure. 8: Percentage of look-angles above the threshold of -95 dBW for arrays optimized using different techniques measured at a distance of 1 km from the transmitter.

As previously discussed, the antenna gain is dependent upon the antenna weights and the steering vector, which in turn depends on the antenna array geometry and the number of antenna elements in the array. In order to see the influence of varying the steering vector on VTL performance, the number of antenna elements and the array geometry were varied, and the weights were computed using the CVX and NM techniques for each case. Different array geometries of linear, square, and circular antenna arrays were investigated. Figure. 9 shows the comparison of various antenna array geometries with 36 antennas and weights computed using different techniques. The CVX optimized array with the relaxed constraint shows more variation with changing geometries compared to the NM optimized array. Also, the arrays symmetric with respect to 2D axes like square and circular arrays perform better than linear arrays that are symmetric with respect to only one axis and this is clearly reflected in Figure. 9.

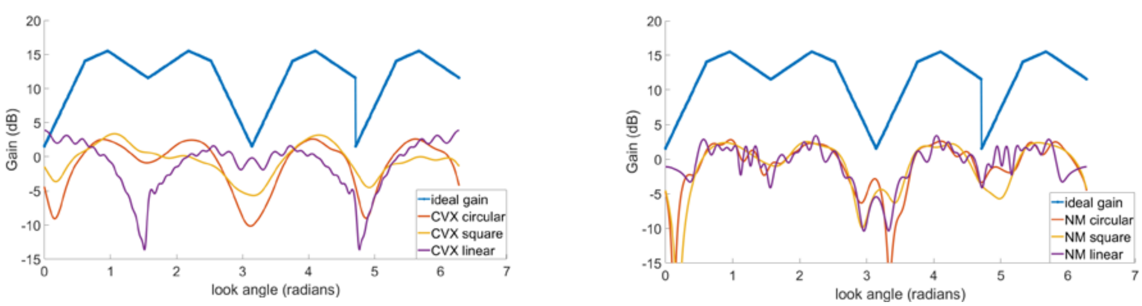

(a) (b)

Figure. 9: Antenna gain patterns for varying array geometries containing 36 elements estimated using (a) convex optimization (b) NM simplex method.

Increasing the number of elements in the array increases the degrees of freedom of an antenna array, thereby, providing an estimate that closely matches the ideal antenna gain. With increasing number of array elements, the maximum directivity of an array in a particular direction also increases. Figure. 10

shows the ideal and the achieved beam patterns of a circular antenna array with varying array elements computed using different optimization methods. It is clear from Figure. 10 that increasing the number of array elements provides a better estimate of the gain pattern.

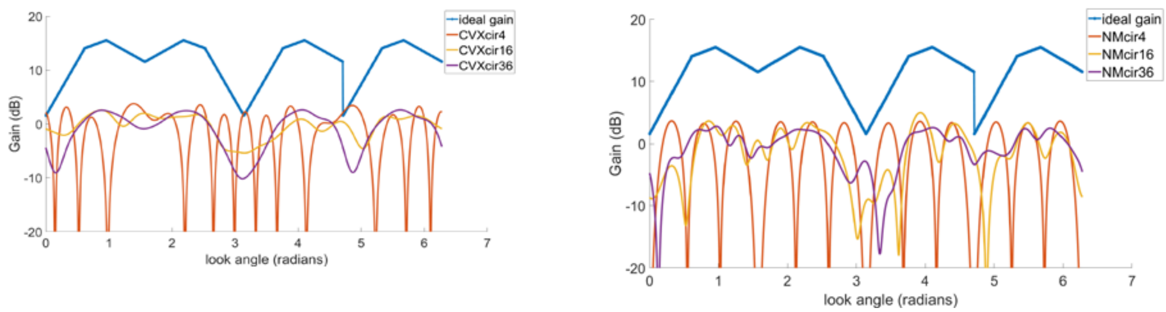

(a) (b)

Figure. 10: Antenna gain patterns of a circular array geometry for varying number of array elements estimated using (a) convex optimization (b) NM simplex method.

As an objective measure of performance, and to complement the graphs in Figure. 9 and Figure. 10, Table 1 and Table 2 show the percentage of look-angles above the threshold of -95 dBW measured at a distance of 1 km from the transmitter with power, $P_t = 10\,W$ for varying antenna array geometries and array elements, respectively.

Table 1. Percentage of look-angles above -95 dBW with varying antenna array geometry (# of antenna elements = 36

Array Geometry	CVX	NM
Linear	46.53	67.36
Square Grid	74.24	83.05
Circular	92.99	79.58

Table 2. Percentage of look-angles above -95 dBW with varying number of antenna elements.

Number of Antenna Elements	CVX	NM
4	56.81	52.53
16	72.64	62.98
36	92.99	79.58

VTL does not perform well with rapidly varying terrain. The passive antenna arrays will not be able to provide variable gain in different directions with abrupt or large changes in terrain. Using active antenna arrays with power amplifiers in the system can improve the response. Figure. 11 shows the comparison of the active antenna gain patterns with the ideal and passive gain patterns. The active antenna weight computation was set up using convex optimization by having the constraint on the weights to be $|w_i| \leq k$, where $k \geq 1$. The power used by the amplifiers is proportional to $|w_i|^2$. Simulations were conducted for the cases when $k = 1, 2, 3$ and the results are shown in Figure. 11. It can be seen that with increasing power, the computed gain patterns move closer to the ideal gain pattern that makes the terrain apparently flat for radio communication.

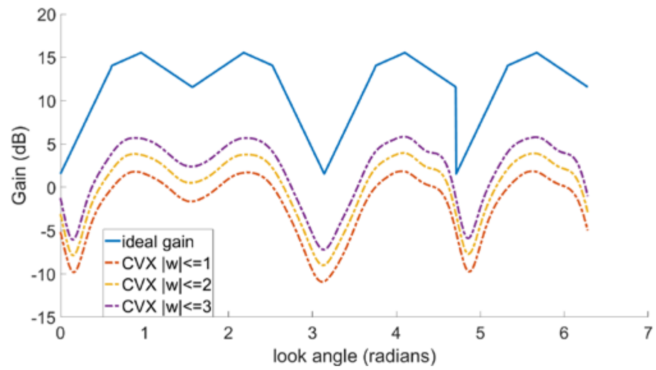

Figure. 11: Antenna gain patterns for increasing amplitude of weights.

5 Conclusion

The novel approach of VTL is proposed that uses phased array antennas to virtually nullify the effects of terrain. The terrain is approximately flattened for radio communication up to the VR from the transmitter. VTL compensates for the communication path losses using antenna array gain. The WIM was used in our simulations for computing the path losses. A hybrid low complexity digital/analog beamforming approach was used for implementing VTL that reduces the hardware cost and complexity of implementation. Two different optimization approaches of using convex optimization and the NM simplex method were employed for estimating the desired beam pattern. The convex optimization approach uses a relaxed constraint to maintain convexity of the problem, whereas, the NM simplex method performs an unconstrained search to find the phase-only weights for the antenna array. The benefits of these two methods can be compared based on the trade-off between increased hardware complexity using convex optimized results, and lower hardware complexity but heavier computational burden of NM.

The power gain of the antenna array was used instead of the normalized array factor to compute the actual received power at a given distance from the transmitter. The gain plots show that the achieved beam patterns try to closely match the ideal beam patterns. The performance of the VTL system was analyzed using the total power injected into the system and the corresponding received power. The percentage of look-angles above the threshold at the receiver was investigated with and without VTL by varying the total power injected into the system and also by increasing the transmitter-receiver separation. VTL shows significant improvement in the percentage of look-angles above the threshold up to the specified VR from the transmitter, and the percentage drops quickly as distance increases. This shows that VTL can potentially mitigate issues like interference in mobile ad hoc networks.

Simulations were conducted to study the benefits of increasing the number of antennas in the array and it was evident from the results that increasing the number of antennas increases the number of degrees of freedom, thereby, providing a better estimate of gain patterns. Various antenna array geometries were also tested and arrays that are symmetric with respect to the 2D axes provided better response compared to linear arrays. One of the limitations of VTL is that it does not perform well in the presence of rapidly varying terrain. Active arrays were also tested and were shown to provide better results in high loss scenarios.

REFERENCES

[1] D. Tate, L. Joneckis, J. Fregeau, C. Kramer and D. Sparrow, "Impact of Terrain Features for Tactical Network Connectivity," Institute for Defense analyses, Alexandria, Virginia, 2013.

[2] J. Pontes, M. Porebska, T. Fugen and W. Wiesbeck, "Base Station Antenna Synthesis for High Sites CDMA Networks," in *European Conference on Antennas & Propagation EUCAP*, Nice, 2006.

[3] J. Pontes, S. Schulteis, M. A. Baldauf and W. Wiesbeck, "Evaluation and Optimization of CDMA System Performance in Macrocell Environments based on Antenna Radiation Pattern.," in *German Microwave Conference*, Karlsruhe, 2006.

[4] J. Pontes, A. Lambrecht, M. Rutschlin, S. Schulteis, M. Porebska, T. Fugen and W. Wiesbeck, "Synthesized Antenna Arrays for Future Mobile Networks.," in *2nd International ITG Conference on Antennas. INICA'07*, 2007.

[5] C. Kosta, B. Hunt , A. U. Quddus and R. Tafazolli, "On interference avoidance through inter-cell interference coordination (ICIC) based on OFDMA mobile systems.," *IEEE Communications Surveys & Tutorials,* vol. 15, no. 3, pp. 973-995, 2013.

[6] S. Y. S. Bhamidipati, "Low Complexity Hybrid Digital/Analog phased array for Ad Hoc networks," University of Wyoming, Laramie, May 2012.

[7] V. B. Ramakrishnaiah, R. F. Kubichek and S. S. Muknahallipatna, "Nelder-Mead Based Iterative Algorithm for Optimal Antenna Beam Patterns in Ad Hoc Networks.," *Journal of Computer and Communications,* vol. 5, no. 07, p. 117, 2017.

[8] V. B. Ramakrishnaiah, R. F. Kubichek and S. S. Muknahallipatna, "Optimization of antenna beam pattern in ad hoc networks for optimal global performance," in *IEEE 58th International Midwest Symposium on Circuits and Systems (MWSCAS)*, Ft. Collins, 2015.

[9] F. Wang, V. Balakrishnan, P. Y. Zhou, J. J. Chen, . R. Yang and C. Frank, "Optimal array pattern synthesis using semidefinite programming.," *IEEE Transactions on Signal Processing,* vol. 51, no. 3, pp. 1172-1183, 2003.

[10] V. B. Ramakrishnaiah, R. F. Kubichek and S. S. Muknahallipatna, "Virtual Terrain Nullification Using Phased Array Antennas for Wireless Ad Hoc Networks," in *The 43nd IEEE Conference on Local Computer Networks (LCN)*, Chicago, USA, October 1-4, 2018.

[11] S. Boyd and L. Vandenberghe, Convex Optimization, Cambridge university press, 2004.

[12] J. A. Nelder and R. Mead, "A simplex method for function minimization," *The computer journal,* vol. 7, no. 4, pp. 308 - 313, 1965.

[13] J. Miles, S. S. Muknahallipatna, R. F. Kubichek, J. McInroy and H. Muralidhara, "Use of radio propagation maps in a single moving beacon assisted localization in MANETs.," in *International Conference on Computing, Networking and Communications (ICNC)*, 2014.

[14] V. B. Ramakrishnaiah, S. S. Muknahallipatna and R. F. Kubichek, "Adaptive Region Construction for Efficient Use of Radio Propagation Maps.," *Journal of Computer and Communications,* vol. 5, no. 8, p. 21, 2017.

[15] D. J. Sadler, "Sector beam synthesis using antenna arrays.," *The IEE Signal Processing Professional Network and EURASIP,* pp. 29/1-5, 2005.

[16] F. J. Ares-Pena, J. A. Rodriguez-Gonzalez, E. Villanueva-Lopez and S. R. Rengarajan, "Ares-Pena, Francisco J., et al. "Genetic algorithms in the design and optimization of antenna array patterns.," in *IEEE Transactions on Antennas and Propagation*, 1999.

[17] S. . Y. S. Bhamidipati, R. F. Kubichek and S. S. Muknahallipatna, "Antenna array geometry for mobile ad-hoc networks.," in *International Conference on Computing, Networking and Communications (ICNC).*, 2014.

[18] J. Walfisch and H. L. Bertoni, "A theoretical model of UHF propagation in urban environments," *IEEE Transactions on antennas and propagation,* vol. 36, no. 12, pp. 1788-1796, 1988.

[19] E. Damosso and L. M. Correia, "Digital Mobile Radio Towards Future Generation Systems Communications. COST 231 Final Report.," CEC, Brussels, Belgium., 1999.

[20] S. J. Orfanidis, Electromagnetic Waves and Antennas., New Brunswick, NJ: Rutgers University, 2002.

[21] S. F. Maharimi, M. F. A. Malek, M. F. Jamlos, S. C. Neoh and M. Jusoh, "Impact of spacing and number of elements on array factor.," in *Proc. of Progress in Electromagnetics ResearchSymposium.*, 2012.

[22] V. B. Ramakrishnaiah, R. F. Kubichek and S. S. Muknahallipatna, "Correction Factor for Power Gain in Antenna Arrays.," *International Journal of Communications, Network and System Sciences,* vol. 11, no. 3, 2018.

[23] S. A. Schelkunoff, "A mathematical theory of linear arrays.," *Bell Labs Technical Journal,* vol. 22, no. 1, pp. 80-107, 1943.

[24] H. G. Booker and P. C. Clemmow, "The concept of an angular spectrum of plane waves, and its relation to that of polar diagram and aperture distribution.," in *Proceedings of the IEE-Part III: Radio and Communication Engineering*, 1950.

[25] P. M. Woodward, "A method of calculating the field over a plane aperture required to produce a given polar diagram.," *Journal of the Institution of Electrical Engineers-Part IIIA: Radiolocation,* vol. 93, no. 10, pp. 1554-1558, 1946.

[26] P. M. Woodward and J. D. Lawson, "The theoretical precision with which an arbitrary radiation-pattern may be obtained from a source of finite size.," *Journal of the Institution of Electrical Engineers-Part III: Radio and Communication Engineering,* vol. 95, no. 37, pp. 363-370, 1948.

[27] O. M. Bucci, G. D'Elia and G. Panariello, "Antenna pattern synthesis: A new general approach.," in *Proceedings of the IEEE*, 1994.

[28] H. Lebret and S. Boyd, "Antenna array pattern synthesis via convex optimization.," in *IEEE transactions on signal processing*, 1997.

[29] M. Grant, "Disciplined Convex Programming," Stanford University, 2004.

[30] M. Grant, S. Boyd and Y. Ye, "Global Optimization: from Theory to Implementation," in *Nonconvex Optimization and Its Applications*, L. Liberti and N. Maculan, Eds., Springer, 2006.

[31] J. C. Lagarias, J. A. Reeds, M. H. Wright and P. E. Wright, "Convergence properties of the Nelder--Mead simplex method in low dimensions," *SIAM Journal on optimization,* vol. 9, no. 1, pp. 112 - 147, 1998.

[32] M. Grant and S. Boyd, "{CVX}: Matlab Software for Disciplined Convex Programming, version 2.1," March 2014. [Online]. Available: http://cvxr.com/cvx.

[33] M. Grant and S. Boyd, "Graph implementations for nonsmooth convex programs," in *Recent Advances in Learning and Control*, V. Blondel, S. Boyd and H. Kimura, Eds., Springer-Verlag Limited, 2008, pp. 95-110.